A continuum model for non-dense growth

2000 J. Phys.: Condens. Matter 12 3195

(http://iopscience.iop.org/0953-8984/12/13/325)

J. Phys.: Condens. Matter **12** (2000) 3195–3217. Printed in the UK PII: S0953-8984(00)07463-4

A continuum model for non-dense growth

J Los†, P Bennema†, P H J van Dam‡, W J P van Enckevort†, F A Hollander† and C N M Keulemans‡

† RIM Laboratory of Solid State Chemistry, University of Nijmegen, Toernooiveld, 6525 ED Nijmegen, The Netherlands

‡ Unilever Research Vlaardingen, Olivier van Noortlaan 120, 3133 AT Vlaardingen, The Netherlands

Received 2 September 1999, in final form 6 December 1999

Abstract. We present a continuum model for diffusion-limited non-dense growth. Our approach leads to a set of two coupled partial differential equations which describe the time evolution of the (spherically) averaged aggregation density and concentration of growth units in the liquid phase. For time-independent parameters the solution of the equations yields a constant (non-fractal) aggregation density. The model gives a phenomenological description of non-fractal unstable growth, e.g. non-fractal spherulitic growth, on a macroscopic scale in terms of a minimal number of parameters and can be used in combination with experimental data, such as the front velocity and the width of the growth front, for both a qualitative and quantitative interpretation of the growth process. The analytical solution of the equations in the diffusion-limited regime leads to simple relations involving the aggregation density and the velocity and width of the growth front. This allows for an easy quantitative analysis of experimental data.

1. Introduction

The growth of branched, non-dense structures has been studied for several decades with the aim of achieving an understanding of unstable crystal growth [1, 2], e.g. dendritic [3–6] and spherulitic growth [7–10], and aggregation processes, such as those of dust and soot [11, 12] and even bacterial colonies [13]. A possible way to model such growth is diffusion-limited aggregation (DLA) [14], a simulation process where growth units are released, one by one, at a point far from the aggregate, make a random walk until they reach the surface of the aggregate and then become part of the aggregate. The structures grown by DLA are non-dense and have a fractal scaling behaviour in the sense that the number of growth units that aggregate within a radius r (for spherical geometry) scales as a non-integer power of r, i.e. $N(r) \propto r^{D_H}$ where D_H is the so-called Hausdorff dimension. The corresponding aggregation density scales then as r^{D_H-d} where d is the 'normal' dimension of the space. For the DLA model in two dimensions starting from a central nucleus, $D_H \simeq 1.7$, independently of the short-range details, such as the symmetry of the underlying lattice and the attachment probability. Since the introduction of the original DLA model, various modifications have been proposed, including incorporation of noise reduction [16, 17], surface kinetics [18], surface diffusion [19] and combinations of these [20, 21], in order to make it more realistic with respect to experimental situations.

Qualitatively the various DLA simulation models are perfect tools for studying unstable growth, but in many cases they are less suitable for a quantitative approach to experimentally observed structures on a macroscopic scale. First, this is due to the fact that the simulation of a real system by means of DLA in a three-dimensional geometry, where a huge number

0953-8984/00/133195+23$30.00

of aggregated units are involved, would require too much computer effort. This is not a simple scaling problem, since the size of the growth units plays an important role as regards characteristics of the aggregate on a macroscopic scale. For instance, the width of the growth front can be as small as the size of one growth unit in the limit of stable growth, and therefore the scaling problem cannot simply be solved by performing, for example, DLA simulations with bigger (pseudo-) growth units and a corresponding scaling of the kinetic and diffusion constants. Secondly, from the DLA simulations, the steady-state limit is often not evident, either because the limit regime has not yet been reached or because there is no steady state. Finally, in many cases there is a strong anisotropy in the adsorption rate as a function of the orientation in which a growth unit is attached. This is often related to the shape of the growth unit, which is far from cubic or spherical in many cases. In particular this holds for the growth of spherulites from chain-like molecules, where a growth unit should be modelled by an elongated rectangular box rather than by the cube which is commonly used in DLA studies. We consider spherulitic growth as a form of unstable growth, although in this case the instability is not primarily associated with a lack of surface free energy, but rather due to a strongly anisotropic growth rate and the occurrence of misoriented branching where the crystallographic orientation of the side branch is different from that of the stem. To model such kinds of growth by means of DLA is far from easy—also because (too) many, often unknown, input parameters are needed for a realistic simulation of the kinetics at the surface and the formation of side branches.

The interest of our model, presented in this paper, is that it provides a tool for making a simple quantitative evaluation of an unstable growth process on the basis of experimentally accessible data, such as the position of the growth front as a function of time, the width of the growth front and the averaged aggregation density. We will not be concerned with the details of the surface kinetics on a microscopic scale, but formulate the problem of diffusion-limited growth with a minimal number of parameters which have a clear relationship with the available experimental data. Therefore our description is phenomenological at the outset and should not be considered as a continuum approach to the DLA model. It cannot predict a fractal dimension. Actually for non-time-dependent parameters the solution of our equations yields a non-fractal dimension, i.e. the aggregation density scales as a constant, implying $D_H = d$. Therefore our model particularly applies to non-fractal diffusion-limited unstable growth. Such growth can occur in a wide variety of molecular systems. An example is given in figure 1, which shows a typical di-sodium oxalate spherulite grown from an aqueous solution. Similar structures can be grown from other simple molecular systems, and also from more complex systems such as proteins. Spherulitic growth also occurs in polymer systems, but in this case it is commonly believed that the growth is largely dominated by the surface kinetics and not by diffusion [22, 23].

The present paper is purely theoretical in the sense that we do not apply our model to any particular experimental system. It presents the theoretical framework of a pragmatic approach to non-dense growth together with indications for how to use it for the interpretation of experiments. Experimental work on non-dense growth which is well described by our model will be reported in a separate paper [24].

Our model, which is derived in section 2, amounts to a coupled set of non-linear partial differential equations, which describe the time evolution of the spherically averaged (or slice averaged in the case of planar geometry) aggregation density as well as the spherically averaged concentration of growth units in the surrounding liquid phase. In section 3 we first present numerical solutions of the equations and then the analytical steady-state solution for different kinds of boundary conditions. In section 4, we show how the model can be applied for the interpretation of experiments. In particular, it leads to a simple test which can be carried out on

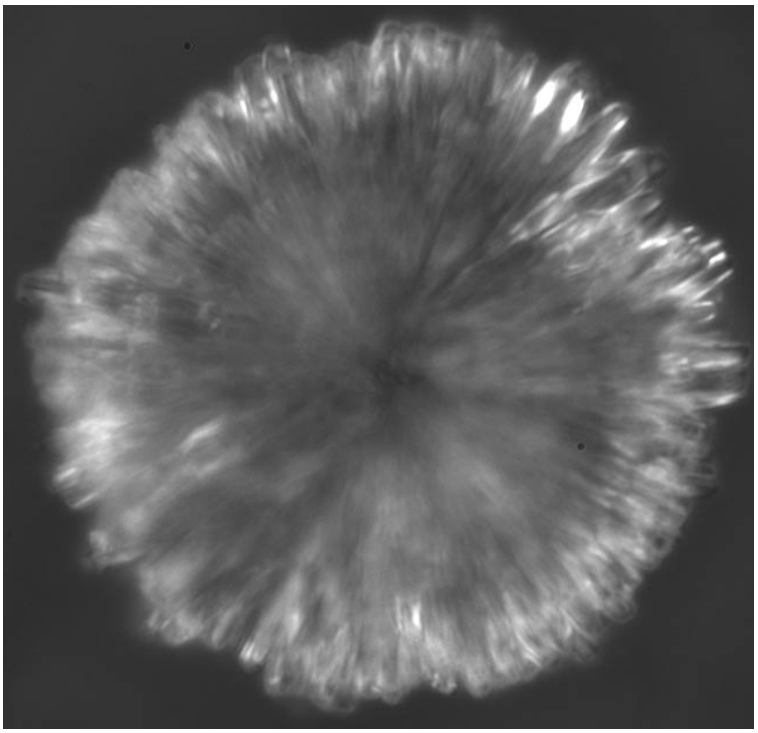

Figure 1. A typical di-sodium oxalate spherulite grown from an aqueous solution.

the basis of front velocity data to find out whether the observed instability is due to diffusion limitation, or to the surface kinetics. To be specific, if it is due to diffusion limitation this means that during the growth the growth units are adsorbed within a relatively small region at the border of the aggregate, the growth front, so they do not reach the inner part of the aggregate which as a consequence remains non-dense. By surface kinetics we mean all mechanisms other than the diffusion in the mother phase, such as the adsorption and desorption of growth units, surface diffusion, growth anisotropy, formation of side branches. Finally, we conclude with a summary and discussion in section 5.

2. Description of the model

For the description of our model, we think of an aggregation process in a bath of diffusing growth units, where the growth of the aggregate takes place by the sticking of these units at the perimeter sites (sites in the liquid adjacent to aggregated growth units) just as in the DLA process. For convenience, in the text we will refer to a spherical geometry ($d = 3$), instead of mentioning each time other possible geometries, such as circular ($d = 2$) and planar ($d = 1$) geometry. The growing aggregate will also be denoted as the solid phase, which is surrounded by the liquid phase.

As a starting point for the derivation of the our equations, we take a generalization of the equations as proposed in reference [14] for a continuum limit description of the DLA process:

$$\frac{\partial \rho}{\partial t} = \frac{u}{\rho_0} \sum_j K_j P_j \tag{1}$$

$$\frac{\partial}{\partial t}\left[\rho + \left(1 - \frac{\rho}{\rho_0}\right)u\right] = -\vec{\nabla}\cdot\vec{J} \tag{2}$$

where $\rho(\vec{r},t)$ and $u(\vec{r},t)$ (both in m^{-3}) are the position- and time-dependent concentrations of growth units in the solid and liquid state of aggregation respectively, and $\vec{J}$ (in $\mathrm{m}^{-2}\ \mathrm{s}^{-1}$) is the growth unit current density defined by

$$\vec{J} = -D\left(1 - \frac{\rho}{\rho_0}\right)\vec{\nabla}u. \tag{3}$$

Actually, since we are dealing with a continuum description, $\rho(\vec{r},t)$ represents the concentration of growth units in the solid state of aggregation per unit of volume, averaged over a small volume that is large compared to the size of one growth unit, so $\rho(\vec{r},t)$ is a smoothed function and has a support between 0 and ρ_0, where ρ_0 (in m^{-3}) is the density of growth units in the completely dense solid phase. Then $1-\rho(\vec{r},t)/\rho_0$ represents the porosity of the structure. $P_j(\vec{r},t)$ (in m^{-3}) is the concentration of perimeter sites of type j, D is the diffusion constant for the transport of growth units in the liquid phase and K_j (in s^{-1}) is the sticking probability per second for the sticking of a growth unit at a perimeter site of type j at a concentration ρ_0 of growth units in the liquid phase and a concentration ρ_0 of perimeter sites. The first expression, equation (1), describes the growth of the solid and the second, equation (2), reflects the conservation of mass. Equation (1) is a generalization with respect to the equation used in reference [14] in the sense that we distinguish between different types of perimeter sites which may have different growth rate constants, whereas in reference [14] all perimeter sites are assumed to be equal. This generalization makes it possible to bring in the anisotropy for cases where the growth rate strongly depends on the orientation of the growth plane. Equation (2) is somewhat different from the corresponding equation in reference [14], due to the fact that it supposes a different definition of u and that it properly takes into account the effect of the excluded volume occupied by the solid, where no diffusion can take place. In our definition of u, the total density of growth units is given by $\rho + (1-\rho/\rho_0)u$, whereas in reference [14] it is equal to $\rho + u$.

For crystal growth from a solution, the growth rate of a (kinetically) roughened surface is proportional to the absolute supersaturation σ defined by

$$\sigma = u - u_{eq} \tag{4}$$

where u_{eq} is the equilibrium concentration of growth units, which is a function of the temperature. Therefore, for the application to crystal growth, u in equation (1) should be replaced by $u - u_{eq}$. In the derivation that follows we have not accounted for such a shift, for convenience. This is a good approximation if u_{eq} is small, but should be kept in mind for larger u_{eq}. The correction related to this shift can be taken into account without complications [24]. Furthermore, besides the mass diffusion one should also consider the heat transport. However, normally the heat transport is much faster than the mass diffusion, so usually one may assume a uniform and constant temperature.

In reference [14] an expansion of the perimeter density in terms of ρ is performed, which leads to a coupled set of non-linear partial differential equations describing the evolution of ρ and u. In principle these equations, with an additional stochastic term to simulate the formation of side branches, could be solved numerically for a given set of suitable starting functions $\rho(\vec{r},0)$ and $u(\vec{r},0)$. However, such a numerical calculation in three dimensions with a highly exotic moving boundary is extremely complicated (if not impossible) and would require considerable computational effort. Moreover, usually there is a lack of information on the values of the various parameters describing the growth kinetics, such as the orientation-dependent growth rate and the probability for non-crystallographic branching. Therefore, we

propose to apply a spherical averaging which reduces the number of space coordinates to one. The resulting set of partial differential equations describe the time evolution of functions that represent quantities which are averaged with respect to the angular coordinates and thus depend only on the radial coordinate r.

We define the averaged solid-phase density, $\tilde{\rho}(r)$, by

$$\tilde{\rho}(r) = \frac{N_s'(r)\,\delta r}{\Omega_d r^{d-1}\,\delta r} \tag{5}$$

where $\Omega_d r^{d-1}\,\delta r$ (with $\Omega_d = 4\pi$ for $d = 3$) is the volume of a spherical shell of radius r and thickness δr and $N_s'(r)\,\delta r$ is the number of growth units in the solid aggregation state within this shell. Here and in the following δr is a number which is very small on a macroscopic scale but larger than the edge length of one growth unit. According to equation (5), $\tilde{\rho}(r)$ has a support between 0 and ρ_0. Next, we define the averaged concentration of growth units in the liquid phase, $\tilde{u}(r)$, by

$$\tilde{u}(r) = \frac{N_l'(r)\,\delta r}{(1-\tilde{\rho}(r)/\rho_0)\Omega_d r^{d-1}\,\delta r} \tag{6}$$

where $N_l'(r)\,\delta r$ is the number of growth units in the liquid phase within the spherical shell between r and $r+\delta r$. The extra factor $(1-\tilde{\rho}(r)/\rho_0)$ accounts for the excluded space occupied by the solid. For $\tilde{\rho}(r,t) = \rho_0$, $\tilde{u}(r)$ is not well defined, but this is not a problem because there is no liquid in a completely dense solid. We assume that the volume per growth unit in the liquid state is equal to that in the solid state, so $\tilde{u}(r)$ has a support between 0 and ρ_0. In most cases this assumption is a good approximation.

With these definitions the growth equation, expression (1), can be rewritten as

$$\frac{\partial\tilde{\rho}(r)}{\partial t} = \frac{\tilde{u}_{surf}(r)}{\rho_0}\sum_j K_j\tilde{P}_j(r) = \frac{\tilde{u}(r)}{\rho_0}\sum_j \tilde{K}_j\tilde{P}_j(r) \tag{7}$$

where $\tilde{u}_{surf}(r)$ is the averaged concentration of growth units at the solid–liquid surfaces at radial position r and $\tilde{P}_j(r)$ is the spherically averaged concentration of perimeter sites of type j defined by

$$\tilde{P}_j(r) = \frac{N_{pj}'(r)\,\delta r}{\Omega_d r^{d-1}\,\delta r} \tag{8}$$

where $N_{pj}'(r)\,\delta r$ is the number of perimeter sites of type j in the liquid phase within the spherical shell between r and $r+\delta r$. If we assume that the concentration of growth units in the liquid is uniform in the lateral directions, i.e. the directions perpendicular to the radial direction, so that $\tilde{u}_{surf}(r) = \tilde{u}(r)$, then the kinetic constants $\tilde{K}_j$ in equation (7) are equal to K_j, defined earlier. This assumption will be a good assumption in many cases for the following reason. Due to the diffusion limitation in the radial direction, the concentration within the growth front will become small (see figure 2) and thus the growth velocity of the crystal faces will also become (relatively) small in the (quasi-) stationary regime. Therefore no strong gradients will be built up over the relatively small lateral distance between the branches. However, if for certain cases the concentration is not uniform in the lateral directions, we may argue that $\tilde{u}_{surf}(r)$ is some factor f smaller than $\tilde{u}(r)$, i.e. $\tilde{u}_{surf}(r) = f\tilde{u}(r)$, where we assume that f is approximately constant within the growth front in the stationary regime or represents an appropriate averaged value. We have included this factor in the kinetic constant $\tilde{K}_j = fK_j$, which is defined as the probability per second of the sticking of a growth unit at a perimeter site of type j at a spherically averaged concentration ρ_0 of growth units in the liquid phase and a spherically averaged concentration ρ_0 of perimeter sites.

The next step that we make is that we assume two kinds of perimeter sites: lateral and parallel perimeter sites. The lateral (or perpendicular) perimeter sites occur at faces parallel to the radial direction and cause the growth in the lateral direction(s), whereas the parallel perimeter sites, occurring at faces perpendicular to the radial direction, cause the growth in the radial direction. This assumption makes sense for unstable growth. A strong lateral growth acts as a stabilizing influence and leads to denser structures. The lateral growth can consist in the thickening of the branches and/or the formation of side branches causing an increase in the number of branches. We note that in reality a perimeter site may be neither purely lateral nor parallel. Such a site will contribute to the perimeter concentrations of both types.

In the limit of small solid-phase density, the lateral perimeter density, $P_\perp(r)$, should be proportional to $\tilde{\rho}(r)$ and is also related to the thickness of the branches. For example, if the number of branches that crosses the sphere of radius r is doubled at equal averaged thickness of the branches, then $P_\perp(r)$ will be twice as large. On the other hand, in the limit of $\tilde{\rho} \to 1$ the lateral perimeter density should vanish. That is, for increasing branch density the branches start to make contact with each other, effectively reducing the growth surface for geometrical reasons. The simplest expression for $P_\perp(r)$, fulfilling the above conditions, is

$$\tilde{P}_\perp(r) = \alpha_b \tilde{\rho}(r)\left(1 - \frac{\tilde{\rho}(r)}{\rho_0}\right). \tag{9}$$

The proportionality constant α_b, which we call the branching factor, is related to the thickness of the branches. One can derive the following estimate for α_b:

$$\alpha_b = \frac{\bar{C}_b(r)\bar{a}_\perp}{\bar{A}_b(r)} \tag{10}$$

where $\bar{C}_b(r)$ and $\bar{A}_b(r)$ are the mean contour and the mean cross section of the branches at their intersection with the sphere of radius r and $\bar{a}_\perp$ is a mean value for the edge lengths in the lateral directions of an adsorbed growth unit. Since $\bar{C}_b \propto \bar{d}_b$ and $\bar{A}_b \propto \bar{d}_b^2$, where $\bar{d}_b$ is the mean diameter of the branches, we have that $\alpha_b \propto 1/\bar{d}_b$ which means that, at equal $\tilde{\rho}(r)$, thin branches yield a larger lateral perimeter concentration than thick branches. We note that the estimate (10) for α_b does not make sense if the aggregate at position r consists of solid phase with liquid channels instead of solid branches surrounded by liquid phase. In this case, which particularly occurs for large solid-phase density, α_b is related to the size of the pores.

The averaged parallel perimeter concentration, $\tilde{P}_\parallel(r)$, is equal to the decrease of the averaged solid-phase density over an interval $a_\parallel$:

$$\tilde{P}_\parallel(r) = -(\tilde{\rho}(r + a_\parallel) - \tilde{\rho}(r)) \simeq -a_\parallel \frac{\partial \tilde{\rho}(r)}{\partial r} \tag{11}$$

where $a_\parallel$ represents the edge length in parallel direction of an adsorbed growth unit.

Corresponding to the perimeter sites of two types, we have two different growth constants, $\tilde{K}_\perp$ and $\tilde{K}_\parallel$. Finally we find, by substitution of equations (9) and (11) into equation (7), the following growth equation:

$$\frac{\partial \tilde{\rho}}{\partial t} = \tilde{K}_\parallel \frac{\tilde{u}}{\rho_0}\left(\alpha \tilde{\rho}\left(1 - \frac{\tilde{\rho}}{\rho_0}\right) - a_\parallel \frac{\partial \tilde{\rho}}{\partial r}\right) \tag{12}$$

where we call α the lateral growth factor, defined by

$$\alpha = \frac{\tilde{K}_\perp}{\tilde{K}_\parallel}\alpha_b \tag{13}$$

where the factor $\tilde{K}_\perp/\tilde{K}_\parallel$ accounts for the anisotropy in the adsorption at lateral and parallel perimeter sites. Although α may vary as a function of r within the growth front, in particular due

to the fact that the averaged thickness of the branches may become larger (and correspondingly α_b smaller) in the inner part of the growth front, we assume an effective constant α which yields the right total lateral growth in the stationary regime.

Furthermore, we also assume that α and $\tilde{K}_\parallel$ are time independent. This assumption implies a restriction of the types of system to which the model applies. Since the steady-state aggregation density is a function of $\tilde{K}_\parallel$ and α, as will be shown below, time-independent parameters yield a constant aggregation density, implying a non-fractal scaling behaviour of $\tilde{\rho}(r)$. In agreement with this, we find a constant width of the growth front.

More generally, we may assume that in the stationary regime, α varies within the growth front as a linear function of ρ, i.e. $\alpha(r,t) = \alpha_0 - \alpha_1 \rho(r,t)$, where we expect α_1 to be positive. However, we have checked numerically that if the variation of α within the growth front is not too large, but e.g. of the order of a factor 2, then the resulting solution is close to the solution for an effective averaged constant α (and equal $\tilde{K}_\parallel$) in the sense that the aggregation density and the width of the growth front both agree approximately. This shows that the dependence of $P_\perp$ on ρ is, apart from the fact that $P_\perp$ should vanish for $\rho = 0$ and $\rho = 1$, not very critical, which justifies the use of an effective constant α as an empirical parameter.

The total flux of growth units in the liquid phase through a sphere of radius r, $J(r)$, is equal to the spherically averaged flux and can be related to the gradient of the spherically averaged concentration by

$$J(r) = D\Omega_d r^{d-1}\left(1 - \frac{\tilde{\rho}}{\rho_0}\right)\frac{1}{\Omega_d}\int \frac{\partial u}{\partial r}\,\mathrm{d}\Omega = D\Omega_d r^{d-1}\left(1 - \frac{\tilde{\rho}}{\rho_0}\right)\frac{\partial \tilde{u}}{\partial r} \tag{14}$$

where in the latter step we have exchanged the integration over the lateral coordinates, represented by Ω, and the differentiation with respect to r. The total quantity of growth units in the liquid phase within a shell with radius r and thickness δr is equal to $\Omega_d r^{d-1}\,\delta r\,(1 - \tilde{\rho}(r)/\rho_0)\tilde{u}$. The rate of change of this quantity is equal to the sum of the fluxes in the liquid phase in and out the shell minus the quantity of growth units that has been adsorbed within the shell:

$$\Omega_d r^{d-1}\,\delta r\,\frac{\partial[(1 - \tilde{\rho}(r)/\rho_0)\tilde{u}(r)]}{\partial t} = J(r + \delta r) - J(r) - \Omega_d r^{d-1}\,\delta r\,\frac{\partial \tilde{\rho}}{\partial t}. \tag{15}$$

If we divide equation (15) by $\Omega_d r^{d-1}\,\delta r$ and take the limit of $\delta r \to 0$, then, by substitution of equation (14), we find the following mass conservation equation:

$$(\rho_0 - \tilde{\rho})\frac{\partial \tilde{u}}{\partial t} = D\left((\rho_0 - \tilde{\rho})\,\nabla_r^2 \tilde{u} - \frac{\partial \tilde{\rho}}{\partial r}\frac{\partial \tilde{u}}{\partial r}\right) - (\rho_0 - \tilde{u})\frac{\partial \tilde{\rho}}{\partial t} \tag{16}$$

where the operator ∇_r^2 stands for

$$\nabla_r^2 = \frac{\partial^2}{\partial r^2} + \frac{d-1}{r}\,\frac{\partial}{\partial r}. \tag{17}$$

It is important to note that, due to the interchangeability of the integration and differentiation as used in expression (14), equation (16) correctly describes the diffusion for the averaged concentration, i.e. it does not contain any further assumptions related to the averaging procedure.

By the scale transformations $\tilde{\rho}' = \tilde{\rho}/\rho_0$ and $\tilde{X} = \tilde{u}/\rho_0$, equations (12) and (16) transform to

$$\frac{\partial \tilde{\rho}}{\partial t} = \tilde{K}_\parallel \tilde{X}\left(\alpha\tilde{\rho}(1 - \tilde{\rho}) - a_\parallel \frac{\partial \tilde{\rho}}{\partial r}\right) \tag{18}$$

and

$$(1 - \tilde{\rho})\frac{\partial \tilde{X}}{\partial t} = D\left((1 - \tilde{\rho})\,\nabla_r^2 \tilde{X} - \frac{\partial \tilde{\rho}}{\partial r}\frac{\partial \tilde{X}}{\partial r}\right) - (1 - \tilde{X})\frac{\partial \tilde{\rho}}{\partial t} \tag{19}$$

where we have dropped the primes for convenience. Hence, in the remainder of this paper, $\tilde{\rho}$ is redefined as the fractional averaged solid-phase density with a support between 0 and 1. Note that $\tilde{X}$ is the fractional averaged concentration of growth units in the liquid phase. In the following, equations (18) and (19) will be referred to as the non-dense growth (NDG) equations.

To solve the NDG equations we need to specify appropriate boundary conditions.

As the initial function $\tilde{\rho}_0(r) \equiv \tilde{\rho}(r, 0)$, representing a nucleus, for the numerical solutions presented below, we have taken a Gaussian-like function which is equal to zero at $r \geqslant R(0)$ where $R(0)$ is the radius of the nucleus, i.e. the radius of the aggregate at $t = 0$. It appears that the solutions of the NDG equations are soliton-like solutions with a sharp kink at $r = R(t)$, where $R(t)$ is the radius of the aggregate at time t (see figure 2) and at the same time the position of the growth front. Mathematically, we define $R(t)$ such that $\tilde{\rho}(r, t) \geqslant \epsilon$ for $r \leqslant R(t)$ and $\tilde{\rho}(r, t) < \epsilon$ for $r > R(t)$, where $\epsilon \ll 1$.

The other initial function, $\tilde{X}_0(r) \equiv \tilde{X}(r, 0)$, has been taken to be the constant function

$$\tilde{X}_0(r) = X_b \tag{20}$$

where X_b is the bulk concentration in the liquid during the growth process.

As regards the concentration of growth units in the liquid phase outside the growth front, we have investigated two different cases.

- *Fixed diffusion layer*: $\tilde{X}(R(t) + \Delta_D, t) = X_b$. Here Δ_D is the width of a fixed (i.e. time-independent) diffusion layer outside the growth front. This boundary condition typically applies to a stirred crystal growth process or in systems where free convection plays an important role.
- *Free diffusion layer*: $\tilde{X}(R(t) + \Delta_D(t), t) = X_b$. This boundary condition means that a diffusion layer is built up during the process with a width $\Delta_D(t)$ which is purely determined by the diffusion process, so $\Delta_D(t)$ is time dependent in general. This boundary condition is realistic for the description of an unstable growth process in a finite system as long as the diffusion layer does not reach the boundaries of the system.

The velocity v of the growth front, i.e. the increase of the radius of the aggregate, resulting from the NDG equations can be derived as follows:

$$v = \frac{\mathrm{d}R}{\mathrm{d}t} \simeq \left.\frac{\partial\tilde{\rho}}{\partial t}\right|_R \left.\frac{\delta R}{\delta\tilde{\rho}}\right|_R \simeq -\left.\frac{\partial\tilde{\rho}}{\partial t}\right|_R \left(\left.\frac{\partial\tilde{\rho}}{\partial r}\right|_R\right)^{-1} \simeq \tilde{K}_\parallel a_\parallel \tilde{X}_R \tag{21}$$

where in last step we have used the growth equation (18) which implies

$$\left.\frac{\partial\tilde{\rho}}{\partial t}\right|_R \simeq -\tilde{K}_\parallel a_\parallel \tilde{X}_R \left.\frac{\partial\tilde{\rho}}{\partial r}\right|_R \tag{22}$$

where we have used that $\tilde{\rho}(R) \leqslant \epsilon$ is very small. In the third step of equation (21), a minus sign appears, since $(\delta R/\delta\tilde{\rho})|_R$ is positive whereas $(\partial\tilde{\rho}/\partial r)|_R$ is negative (see figure 2). Equation (20) shows that the front velocity is proportional to the averaged concentration of growth units at the growth front, $\tilde{X}_R$, as it should be since we have assumed linear growth kinetics. The proportionality constant, $\tilde{K}_\parallel a_\parallel$, is just the growth velocity per unit of fractional averaged concentration, $\hat{v}$, so

$$\tilde{K}_\parallel = \frac{\hat{v}}{a_\parallel}. \tag{23}$$

Usually, experimental values or estimates of $\hat{v}$ and $a_\parallel$ are available as input.

3. The solutions

To find the solutions of the NDG equations we first apply the following scale transformations to the dimensionless coordinates:

$$r' = \sqrt{\frac{\alpha \hat{v}}{D a_{\parallel}}} r \tag{24}$$

and

$$t' = \frac{\alpha \hat{v}}{a_{\parallel}} t. \tag{25}$$

By this transformation and using equation (23) the NDG equations (18) and (19) transform to

$$\frac{\partial \tilde{\rho}}{\partial t} = \tilde{X}\left(\tilde{\rho}(1-\tilde{\rho}) - \lambda \frac{\partial \tilde{\rho}}{\partial r}\right) \tag{26}$$

and

$$(1-\tilde{\rho})\frac{\partial \tilde{X}}{\partial t} = \left((1-\tilde{\rho})\,\nabla_r^2 \tilde{X} - \frac{\partial \tilde{\rho}}{\partial r}\frac{\partial \tilde{X}}{\partial r}\right) - (1-\tilde{X})\frac{\partial \tilde{\rho}}{\partial t} \tag{27}$$

where we have omitted the primes for convenience and where the only remaining parameter λ is defined by

$$\lambda = \sqrt{\frac{\hat{v} a_{\parallel}}{\alpha D}}. \tag{28}$$

We call λ the instability parameter. As we will see below, a large λ yields an open structure with a low solid-phase density, whereas a small λ gives a dense structure. Note that λ contains both the surface kinetics, represented by $\hat{v}$ and α, and the mass diffusion, represented by D.

In the next section we will first consider numerical solutions of equations (26) and (27) and then, in section 3.2, we present the analytical steady-state solution.

3.1. Numerical solutions

In figure 2 typical solutions for $d = 3$ (i.e. spherical geometry) and a *free diffusion layer* with $X_b = 0.1$ are shown for $\lambda = 0.5$, 1.5 and 2.5. Clearly the instability parameter λ controls the averaged solid-phase density. For a given t three regions can be distinguished along the space axis: a starting region OA, a static region AB and a front region BC (see figure 2(b)). In the regions OA and AB the concentration of growth units in the liquid phase has dropped to zero, so the growth only takes place in the front region BC, which is called the growth front. By numerical analysis we found that in the region AB, $\tilde{\rho}(r)$ behaves as

$$\tilde{\rho}(r) = \tilde{\rho}_s + \frac{A}{r} \tag{29}$$

where A is a constant depending on λ and X_b. The second term in equation (29) is a small correction which vanishes for large r and occurs only for $d = 2$ and $d = 3$ and not for $d = 1$. Apparently it is due to the $(d-1)/r$ term in expression (17) for the ∇_r^2 operator. In fact the $1/r$ correction is relatively unimportant. In the static region the solid-phase density is almost constant and equal to $\tilde{\rho}_s$. This corresponds to a structure with a uniform distribution of the solid phase. For a free diffusion layer, considered here, the value of $\tilde{\rho}_s$ depends only on the instability parameter λ and not on X_b as long as $\tilde{\rho}_s$ is larger than X_b. For increasing λ and fixed X_b, $\tilde{\rho}_s$ decreases until, at some critical λ, it becomes equal to X_b and then remains constant. This agrees with the fact that mass transport is no longer a limiting factor if the

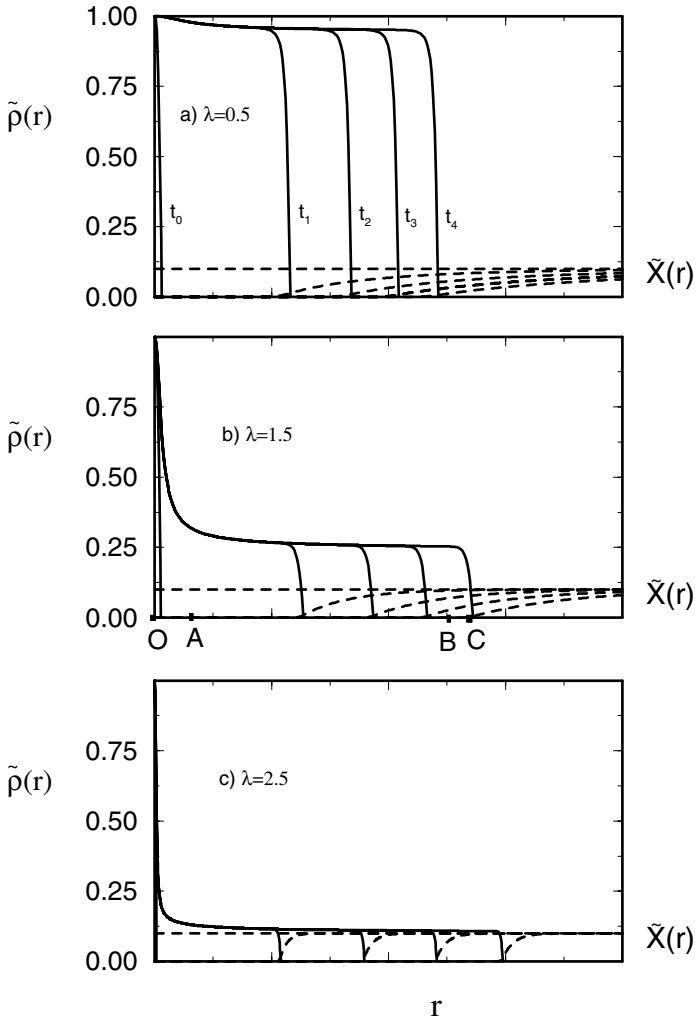

Figure 2. The evolution of the averaged solid-phase density $\tilde{\rho}(r)$ and concentration of growth units in the liquid phase, $\tilde{X}(r)$, as a function of r (in dimensionless units) over equidistant times $t_0, \ldots, t_4$ obtained by numerically solving equations (26) and (27) for (a) $\lambda = 0.5$, (b) $\lambda = 1.5$ and (c) $\lambda = 2.5$ and a free diffusion layer with $X_b = 0.1$.

solid-phase density does not exceed the liquid bulk concentration of the growing substance. Thus $\tilde{\rho}_s \in [X_b, 1]$. An analytical expression for $\tilde{\rho}_s$, obtained from the steady-state solution, will be given below.

Besides this, we also found that $\tilde{\rho}_s$ was dependent on the choice of the finite-difference interval of the numerical solution. Normally one should reduce the size of this interval until convergence is achieved. However, for small λ it was difficult to achieve convergence. Reducing the size of the finite-difference interval, the solutions did not change qualitatively but the value of $\tilde{\rho}_s$ slightly increased. The reason for this is that the width of the growth front vanishes for small λ, as will be clear from the analytical steady-state solution presented in section 3.2, and the fact that it is hardly possible to describe a completely sharp interface in a finite-difference method. Therefore we have made a fixed choice for the finite-difference

interval δr and taken it equal to $\lambda/2$. Qualitatively, this choice does not change the results shown of figure 2, as is also confirmed by the analytical solution.

The velocity of the front, $v(t)$, divided by the initial velocity $v_0 = v(0)$ is shown in figure 3 for $X_b = 0.1$ and two values of λ. In the dimensionless coordinate system the velocity of the front is given by applying the scale transformations (24) and (25) to equation (21):

$$v(t) = \tilde{X}_R(t)\lambda \tag{30}$$

where we have also used equations (23) and (28). Initially, at $t = 0$, the concentration at the front, $\tilde{X}_R(0)$, still equals the bulk concentration, X_b, so the initial velocity is equal to $v_0 = X_b\lambda$. Then, after the growth process has started, there is a rapid collapse of the velocity, but soon a quasi-stationary regime is entered where the velocity decreases only weakly. By plotting $\ln(v)$ versus $\ln(t)$ we found a straight line with a slope of $-1/2$ for large t, which means that $v(t)$ behaves as $t^{-1/2}$ for large t, i.e. after the initial collapse. At least this is the case for values of λ where $\tilde{\rho}_s$ is larger than X_b. The $t^{-1/2}$-behaviour is typical for diffusion-limited growth [2]. An empirical expression that gives the correct front velocity at $t = 0$ and fits quite well with the numerically obtained front velocity for the case where $\tilde{\rho}_s > X_b$ is given by

$$v(t) = \frac{X_b\lambda}{\sqrt{1 + B_v t}} \tag{31}$$

with a suitable constant B_v. The agreement of expression (31) with the numerical solution is illustrated by the dashed lines in figure 3. For sufficiently long times we have that $B_v t$ is much larger than one. In this limit the front velocity tends to

$$v_s(t) = \frac{X_b\lambda}{\sqrt{B_v t}}. \tag{32}$$

This is the front velocity in the diffusion-limited regime. In the next section an analytical expression for B_v will be derived.

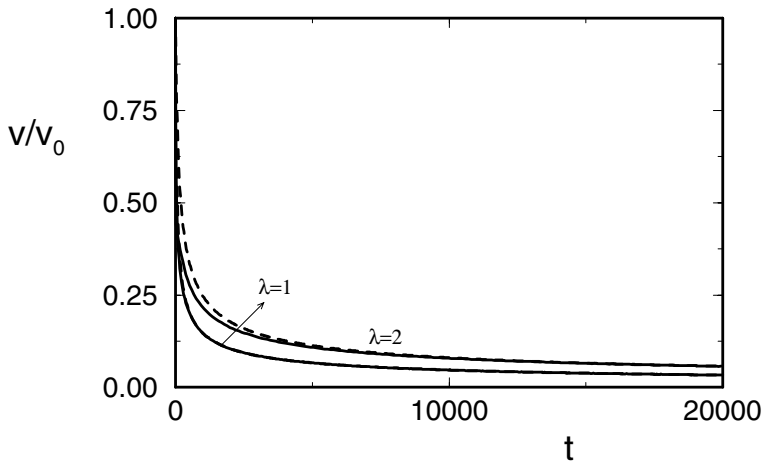

Figure 3. The front velocity v divided by the initial velocity $v_0 = X_b\lambda$ as a function of time (in dimensionless units) for $\lambda = 1$ and 2 and a free diffusion layer with $X_b = 0.1$.

For large values of λ, where $\tilde{\rho}_s = X_b$, the front velocity decreases at the beginning, but soon a stationary situation is reached where it remains constant.

For a *fixed diffusion layer* of width Δ_D, where $\tilde{X}(R(t) + \Delta_D, t) = X_b$, numerical analysis shows that the behaviour of $\tilde{\rho}(r)$ as a function of r is equal to that for a free diffusion layer

and is described by the expression (29). For large Δ_D the value of $\tilde{\rho}_s$ is almost equal to that for a free diffusion layer, but a higher $\tilde{\rho}_s$ occurs for small Δ_D in particular for large X_b (see the next section). Initially, the front velocity behaves according to equation (31), but after a short time it remains constant in contrast to the $t^{-1/2}$-behaviour for a free diffusion layer.

If the system is taken to be finite, this has no effect on $\tilde{\rho}(r)$, but the front velocity starts to decrease rapidly when the diffusion layer reaches the boundary of the system.

3.2. Analytical steady-state solution

The numerical solutions of the NDG equations for a fixed diffusion layer show that there is a steady-state solution with a constant front velocity in this case. In this section this solution is derived analytically, leading to expressions for $\tilde{\rho}_s$, the front velocity and the width of the growth front. Then the solutions are adapted for the case of a free diffusion layer, which leads to an analytical determination of the coefficient B_v defined above.

3.2.1. Fixed diffusion layer. To find the steady-state solution in the case of a fixed diffusion layer, yielding a constant front velocity v in the stationary regime, we apply the following coordinate transformation:

$$z = r - vt \tag{33}$$

and choose the origin in the moving frame at the growth front, i.e. $z = 0$ at $r = R$. This transformation implies the following replacements in equations (26) and (27):

$$\frac{\partial}{\partial t} \to -v\frac{\mathrm{d}}{\mathrm{d}z} \qquad \text{and} \qquad \frac{\partial}{\partial r} \to \frac{\mathrm{d}}{\mathrm{d}z}. \tag{34}$$

Then, after some algebra and using the fact that the term proportional to $1/r$ vanishes in the stationary regime, equations (26) and (27) can be rewritten as

$$\dot{\tilde{\rho}} = \frac{\tilde{X}\tilde{\rho}(1-\tilde{\rho})}{\lambda\tilde{X} - v} \tag{35}$$

and

$$\dot{\tilde{\rho}} = \frac{(1-\tilde{\rho})\ddot{\tilde{X}} + v(1-\tilde{\rho})\dot{\tilde{X}}}{v\tilde{X} + \dot{\tilde{X}} - v} \tag{36}$$

respectively, where the dots and double dots indicate the first and the second derivatives with respect to z respectively. For $z \geqslant 0$, where $\tilde{\rho}$ is zero, it follows from equation (36) that $\tilde{X}(z)$ is a solution of

$$\ddot{\tilde{X}} = -v\dot{\tilde{X}} \qquad (z > 0). \tag{37}$$

The boundary conditions for $\tilde{\rho}(z)$ and $\tilde{X}(z)$ are: $\tilde{\rho}(0) = 0$, $\tilde{X}(0) = \tilde{X}_R = v/\lambda$, $\tilde{X}(-\infty) = 0$ and $\tilde{X}(\Delta_D) = X_b$.

For $z < 0$, where $\tilde{\rho}(z) > 0$, the right-hand side of equation (35) must be equal to that of equation (36), which leads to a quadratic equation for $\tilde{\rho}$ with two solutions. One of the solutions is given by

$$\tilde{\rho} = \frac{(\lambda\tilde{X} - v)(\ddot{\tilde{X}} + v\dot{\tilde{X}})}{\tilde{X}(v\tilde{X} + \dot{\tilde{X}} - v)} \tag{38}$$

and the other one is the constant function $\tilde{\rho} = 1$. Consider the former solution. By substitution of equation (38) into equation (35) we obtain an uncoupled differential equation for $\tilde{X}$, which has a simple solution satisfying the above-mentioned boundary conditions, namely

$$\tilde{X}(z) = \tilde{X}_R \exp(z/\lambda) = \frac{v}{\lambda}\exp(z/\lambda) \qquad (z < 0). \tag{39}$$

Substitution of this $\tilde{X}(z)$ into equation (38) leads to

$$\tilde{\rho}(z) = \frac{C(1 - \exp(z/\lambda))}{C(1 - \exp(z/\lambda)) + 1} \qquad (z < 0) \tag{40}$$

where C is given by

$$C = \frac{1 + \lambda v}{\lambda^2 - 1 - \lambda v}. \tag{41}$$

The value of $\tilde{\rho}_s$ as defined above is given by the value of $\tilde{\rho}(z)$ for $z \to -\infty$:

$$\tilde{\rho}_s = \frac{1 + \lambda v}{\lambda^2} = \frac{1}{\lambda^2} + \tilde{X}_R. \tag{42}$$

Since $\tilde{\rho}_s$ must be less than or equal to one, the solution (40) is only acceptable if $\lambda^2 > 1 + \lambda v$. The concentration of growth units at the growth front will be smaller than the bulk concentration, i.e. $\tilde{X}_R \leqslant X_b$. Therefore the contribution of the second term on the right-hand side of equation (42) is maximally equal to X_b. The value of $\tilde{X}_R$ is, by equation (30), directly related to the front velocity, which we have still not determined but which will be given below. A relatively large front velocity, i.e. a large $\tilde{X}_R$, occurs for a small diffusion layer, and thus a significant increase of $\tilde{\rho}_s$ can occur for large X_b and a small fixed diffusion layer. For the case of a free diffusion layer, which is treated further on, the term $\tilde{X}_R$ in equation (42) can be neglected if $\tilde{\rho}_s > X_b$, i.e. if $\lambda < \sqrt{1/X_b}$. We note that, particularly for small λ, the result of equation (42) is quantitatively not in agreement with the numerical results shown in figure 2, which is due to the bad convergence of the numerical solution as a function of the finite-difference step length as explained above.

For $\lambda^2 \leqslant 1 + \lambda v$, the physically relevant solution is given by the other solution of equations (35) and (36), i.e. $\tilde{\rho} = 1$, implying

$$\tilde{\rho}(z) = \theta_-(z) \tag{43}$$

where $\theta_-(z)$ is equal to zero for $z \geqslant 0$ and one for $z < 0$. The solution (43) represents a completely dense structure with a sharp interface of zero width. Actually in the limit of $\lambda^2 \downarrow 1 + \lambda v$ the solution (40) converges to the solution (43). In this limit, C tends to infinity and $\tilde{\rho}(z)$ becomes equal to one for all $z < 0$.

For $z \geqslant 0$, $\tilde{\rho}(z) = 0$ and the solution of equation (37) that satisfies the boundary conditions is given by

$$\tilde{X}(z) = \left(\frac{X_b - \tilde{X}_R}{1 - \exp(-v\Delta_D)}\right)(1 - \exp(-vz)) + \tilde{X}_R \qquad (z \geqslant 0). \tag{44}$$

In the case where $\lambda^2 > 1 + \lambda v$, where $\tilde{\rho}(z)$ is given by expression (40) for $z < 0$, the solution for $\tilde{X}(z)$ is continuous at $z = 0$, since both expressions (39) and (44) yield $\tilde{X}(0) = \tilde{X}_R$. Furthermore, one can show by integration of equation (36) over an infinitesimal interval across the interface (i.e. around $z = 0$) that also $\dot{\tilde{X}}(z)$ must be continuous at $z = 0$. This flux continuity constraint, i.e. equating the derivatives of equations (39) and (44) at $z = 0$, and using the fact that $\tilde{X}_R = v/\lambda$, leads to the following transcendental equation for the front velocity:

$$v = \lambda X_b - \frac{1}{\lambda}(1 - \exp(-v\Delta_D)) \tag{45}$$

which fixes the value of v for a given diffusion layer width Δ_D. For $\Delta_D = 0$ we find that $v = \lambda X_b$ and $\tilde{X}_R = X_b$ as it should.

If instead the solution for $\tilde{\rho}$ is given by the step function (43) (for $\lambda^2 \leqslant 1 + \lambda v$), then $\tilde{X}(z)$ is not defined for $z < 0$ (inside a completely dense structure!), but for $z \geqslant 0$ the solution

(44) for $\tilde{X}(z)$ still applies. In this case the value of v follows from the constraint that the total flux through the interface at $z = 0$ must be equal to the velocity times the averaged density:

$$\left.\frac{\mathrm{d}\tilde{X}}{\mathrm{d}z}\right|_0 + v\tilde{X}_R = v\tilde{\rho}_s \tag{46}$$

with $\tilde{\rho}_s$ equal to one in this case. The first term on the left-hand side represents the current of growth units passing the interface and the second term represents the extra quantity of growth units that passes the interface due to the fact that the interface is moving. We note that equation (46) also applies if $\lambda^2 > 1 + \lambda v$. However, in that case we have to substitute equation (42) for $\tilde{\rho}_s$ and get back to equation (45). Working out equation (46) with $\tilde{\rho}_s = 1$ leads to

$$v = \lambda - \lambda(1 - X_b)\exp(v\Delta_D) \tag{47}$$

where we have used the fact that $\tilde{X}_R = v/\lambda$. Again, $v = \lambda X_b$ for $\Delta_D = 0$.

In figure 4 the value of $v/v_0 = v/(X_b\lambda)$ is shown as a function of Δ_D for various values of λ and X_b. Depending on the value of λ, the value of v has been calculated according to equation (45) or equation (47).

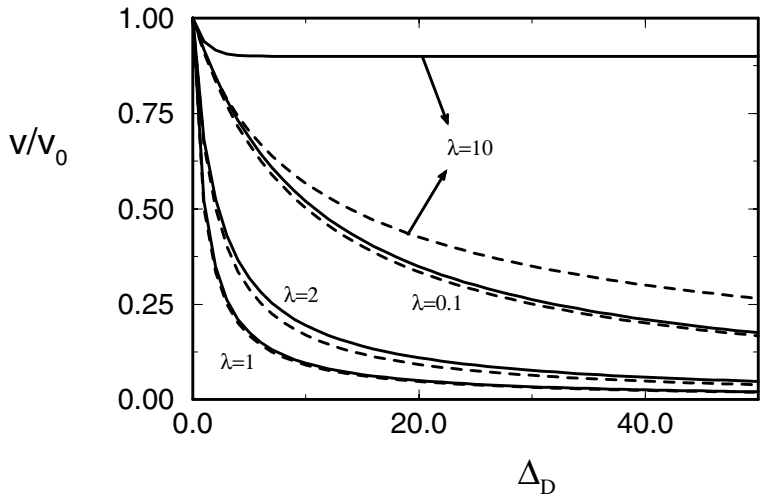

Figure 4. The front velocity v divided by the initial velocity $v_0 = X_b\lambda$ as a function of a fixed diffusion layer width Δ_D for $\lambda = 0.1$, 1, 2 and 10 and $X_b = 0.1$ (full curves) and 0.01 (broken curves).

For a given $\lambda > 1$, expression (40) is the solution for $\tilde{\rho}(z)$ if $\lambda^2 > 1 + \lambda v$, implying $v < (\lambda^2 - 1)/\lambda$. Due to equation (45), this implies the following condition for Δ_D:

$$\Delta_D > -\left(\frac{\lambda}{\lambda^2 - 1}\right)\ln[(1 - X_b)\lambda^2]. \tag{48}$$

If this condition is not satisfied, then the physically relevant solution for $\tilde{\rho}(z)$ is given not by equation (40) but by the step function (43). For $\lambda^2 > 1/(1 - X_b)$, condition (48) is always fulfilled and the relevant solution is given by equation (40) for any value of Δ_D. Vice versa, equation (48) defines a relation for the critical value of λ, which we denote as λ_c, where the growth becomes non-dense as a function of Δ_D. For $\lambda > \lambda_c$ the growth is non-dense, i.e. $\tilde{\rho}_s < 1$. Figure 5 shows λ_c as a function of Δ_D for various values of X_b.

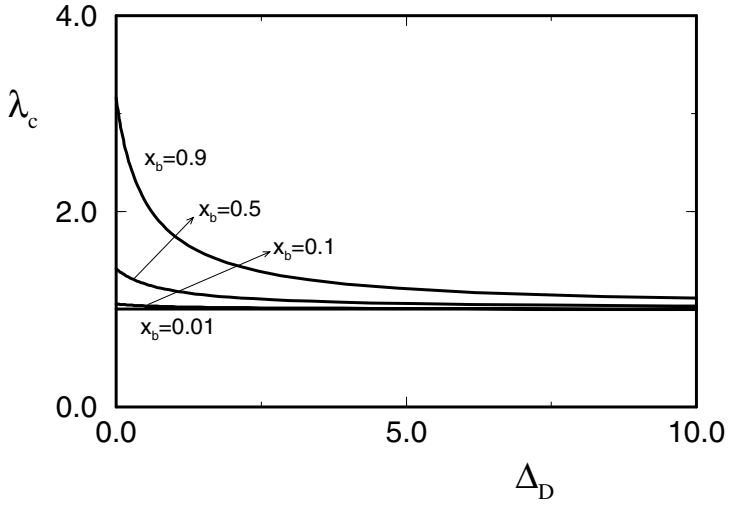

Figure 5. The critical value of λ, λ_c, at which the transition from stable growth ($\lambda \leqslant \lambda_c$) to unstable growth ($\lambda > \lambda_c$) takes place according to the NDG equations as a function of the fixed layer width Δ_D (in dimensionless units) and for four values of X_b. In the case of a free diffusion layer, $\lambda_c = 1$ for any $X_b < 1$.

From equation (45) we can derive the following bounds for the value of v:

$$\lambda X_b - \frac{1}{\lambda} < v < \lambda X_b. \tag{49}$$

For large λ the term $\exp(-v\Delta_D)$ in equation (45) vanishes rapidly for finite non-zero Δ_D, and v tends to

$$v \simeq \lambda X_b - \frac{1}{\lambda}. \tag{50}$$

By substitution of this v into equation (42) we find that $\tilde{\rho}_s$ is equal to X_b such values of λ. In the case where $\Delta_D = 0$ we have that $v = \lambda X_b$ and find that $\tilde{\rho}_s$ is equal to $(1+\lambda^2 X_b)/\lambda^2$, which again converges to X_b for $\lambda \to \infty$. So we find that X_b is a lower bound for $\tilde{\rho}_s$ in agreement with the numerical result.

If we define the penetration depth as the distance where the concentration of growth units in the liquid phase inside the aggregate has dropped to $1/\mathrm{e}$ times its value at the front, then according to equation (39) the penetration depth is equal to λ.

We define the front width Δ_G as the distance between the front and a point inside the aggregate where the averaged solid-phase fraction is equal to a fraction $(1 - \exp(-1))$ times the limit value $\tilde{\rho}_s$, i.e.

$$\tilde{\rho}(-\Delta_G) = (1 - \exp(-1))\tilde{\rho}_s \tag{51}$$

which can be worked out and leads to

$$\Delta_G = \lambda[1 + \ln(\exp(-1)\tilde{\rho}_s + 1 - \tilde{\rho}_s)] \tag{52}$$

where we have used equations (40), (41) and (42). Equation (52) gives a monotonic relation between the front width and the density $\tilde{\rho}_s$. Note that for a given v, λ is also a function of $\tilde{\rho}_s$ by equation (42). We find that $\Delta_G = 0$ for $\tilde{\rho}_s = 1$ and $\Delta_G = \lambda$ for $\tilde{\rho}_s \to 0$ (only possible for $X_b \to 0$). More generally, instead of the fraction $(1 - \exp(-1))$ in equation (51), one can take $(1 - \exp(-n))$ with n a positive integer, yielding $\Delta_G = 0$ for $\tilde{\rho}_s = 1$ and $\Delta_G = n\lambda$ for

$\tilde{\rho}_s \to 0$. If the front width is available from experimental data, then the choice of n has to be in agreement with the definition and/or the accuracy of the experimental front width. In figure 6, Δ_G/λ is shown as a function of $\tilde{\rho}_s$, according to equation (52) and for $n = 1, 2$ and 3.

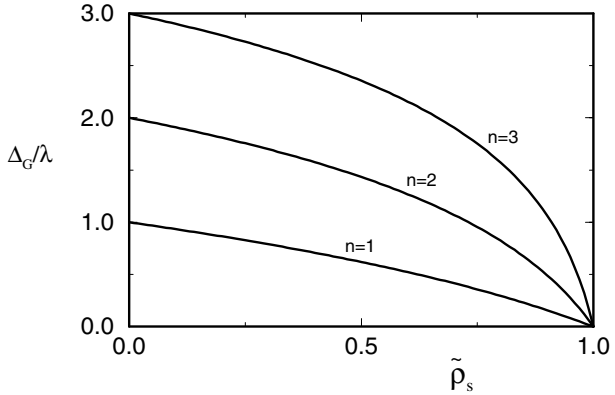

Figure 6. The width of the growth front, Δ_G (in dimensionless units), divided by λ as a function of the averaged density in the static region, $\tilde{\rho}_s$, for $n = 1, 2$ and 3 (see the text).

3.2.2. Free diffusion layer. If the diffusion layer width Δ_D is not kept constant by some external process (e.g. agitation or stirring) and the averaged solid-phase density is larger than the bulk concentration of growth units in the liquid phase, then Δ_D will increase in time. Consequently the concentration of growth units at the front and thus the front velocity will decrease in time. Therefore, to find the solutions for large t, i.e. in the the quasi-stationary regime, we apply the more general transformation

$$z = r - R(t) \tag{53}$$

so, instead of the replacements (34), we have to make the following replacements in equations (26) and (27):

$$\frac{\partial}{\partial t} \to \frac{\partial}{\partial t} - v(t)\,\frac{\partial}{\partial z} \qquad \text{and} \qquad \frac{\partial}{\partial r} \to \frac{\partial}{\partial z} \tag{54}$$

where $v(t) = \mathrm{d}R/\mathrm{d}t$ is the time-dependent front velocity. However, in the limit of large t, and assuming that the front velocity behaves as $v(t) \propto t^{(\beta-1)}$ with $0 < \beta < 1$ for large t, the solutions (39), (40), (43) and (44) with v replaced by $v(t)$ still apply, because by substitution of these solutions into the differential equations we find that the extra terms due to the partial derivative $\partial/\partial t$ are at least a factor $t^{-\beta}$ smaller than the highest-order terms.

From the numerical solution we found that the exponent β is equal to 1/2. Here we will show analytically that this is indeed the correct exponent. Generally we may assume the following power-law behaviour for $R(t)$ and $\Delta_D(t)$ in the quasi-stationary regime:

$$R(t) \simeq B_R t^{\beta} \Rightarrow v(t) = \beta B_R t^{(\beta-1)} \tag{55}$$

and

$$\Delta_D(t) \simeq B_\Delta t^{\gamma} \tag{56}$$

where B_R and B_Δ are independent of time.

In the following analysis we consider the case where $1 < \lambda < \sqrt{1/X_b}$, i.e. the case where the growth is non-dense and $\tilde{\rho}_s > X_b$, and determine B_R and B_Δ for this case after first

showing that $\beta = \gamma = 1/2$. Since for $\tilde{\rho}_s > X_b$ the concentration of growth units in the liquid phase at the growth front vanishes in the quasi-stationary regime, we may neglect the second term in equation (42), so $\tilde{\rho}_s = 1/\lambda^2$ for $\lambda > 1$.

As for a fixed diffusion layer, $\partial \tilde{X}/\partial z$ must be continuous at $z = 0$. Therefore equation (45) remains valid for large t, where it approaches

$$\exp(-v(t)\Delta_D(t)) = 1 - \lambda^2 X_b \tag{57}$$

since $v(t)$ is smaller by a factor $t^{\beta-1}$ than the constant terms. This relation can only be satisfied if the right-hand side is positive, i.e. if $\lambda < \sqrt{1/X_b}$. In the limit of $\lambda \uparrow \sqrt{1/X_b}$, the density $\tilde{\rho}_s$ tends to the value X_b. For $\lambda \geqslant \sqrt{1/X_b}$, $\tilde{\rho}_s$ is equal to X_b, and $v(t)$ does not vanish for large t but remains constant. In this case, equation (57) does not apply, but v follows from equation (45) with an appropriate Δ_D that follows from the total mass conservation (given by equation (59) below). This result is completely reasonable, because if the density of the solid phase does not exceed the bulk concentration of growth units in the liquid phase, mass transport is no longer a limiting factor and the velocity will not decrease over time in the stationary regime.

For $\lambda < \sqrt{1/X_b}$, it follows from equation (59) that $v(t)\Delta_D(t)$ must be a constant for $t \to \infty$. Using equations (55) and (56) this implies the following relation for the exponents β and γ:

$$\beta + \gamma = 1. \tag{58}$$

A second relation for β and γ is obtained by imposing global conservation of mass which, assuming an initial situation with only growth units in the liquid phase with a constant concentration X_b, implies

$$\int_0^{R(t)} (\tilde{\rho}_s - X_b) r^{d-1}\, \mathrm{d}r + \int_{R(t)}^{R(t)+\Delta_D(t)} (\tilde{X} - X_b) r^{d-1}\, \mathrm{d}r = 0 \tag{59}$$

where we have assumed that the width of the initial regime and the growth front is much smaller than $R(t)$, which is always the case for sufficiently large t. To carry out the integrations in equation (59) we substitute $\tilde{\rho}_s = 1/\lambda^2$ and approximate $\tilde{X}(r, t)$ for $r \geqslant R(t)$ by

$$\tilde{X}(r, t) = \frac{X_b}{(1 - \exp(-v\Delta_D))}(1 - \exp(-vz)) = \frac{1}{\lambda^2}(1 - \exp(-v(r - R(t))) \tag{60}$$

where we have used the fact that $\tilde{X}_R = v/\lambda$ becomes negligible with respect to X_b in the quasi-stationary regime and equation (57). With these substitutions, for the case of planar geometry ($d = 1$), equation (59) leads to

$$(1 - q)(R + \Delta_D) - \frac{q}{v} = 0 \tag{61}$$

where q is defined by

$$q \equiv \lambda^2 X_b. \tag{62}$$

By substitution of equations (55) and (56) into equation (61) we find that equation (61) can only be satisfied for all t if β is equal to γ, which together with equation (58) leads to

$$\beta = \gamma = 1/2. \tag{63}$$

We note that equation (63) is also valid for $\lambda \leqslant 1$, where $\tilde{\rho}_s = 1$.

Equation (57) yields the following relation between v and Δ_D:

$$\Delta_D = -\frac{C_q}{v} \tag{64}$$

where C_q is equal to

$$C_q = \ln(1-q). \tag{65}$$

By substitution of equation (64) into equation (61) and using equation (55) we find

$$B_R^2 = \frac{2q}{1-q} + 2C_q. \tag{66}$$

Combination of equations (55), (56), (63) and (64) gives

$$B_\Delta = -\frac{2C_q}{B_R}. \tag{67}$$

For circular ($d = 2$) and spherical ($d = 3$) geometry the procedure for finding B_R and B_Δ is exactly the same and can also be worked out analytically. Equation (63) applies to all d. For $d = 2$ we find that B_R^2 is the solution of a polynomial of the second degree in B_R^2 yielding

$$B_R^2 = 2\left(\frac{q}{1-q} + C_q\right) + 2\left[\left(\frac{q}{1-q}\right)^2 + \frac{2(C_q+q)}{1-q}\right]^{1/2}. \tag{68}$$

For $d = 3$, B_R^2 is the solution of a polynomial of the third degree in B_R^2:

$$B_R^6 + a_4 B_R^4 + a_2 B_R^2 + a_0 = 0 \tag{69}$$

where

$$a_4 = -6\left(\frac{q}{1-q} + C_q\right) \tag{70}$$

$$a_2 = -12\left(\frac{2q}{1-q} + 2C_q - C_q^2\right) \tag{71}$$

$$a_0 = -8\left(\frac{6q}{1-q} + 6C_q - 3C_q^2 + C_q^3\right). \tag{72}$$

In figure 7, B_R is shown as a function of q for $d = 1$, 2 and 3. Equation (67) for B_Δ applies to $d = 1$, 2 and 3.

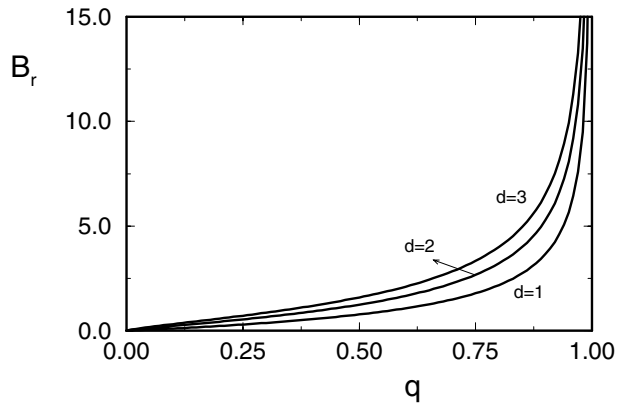

Figure 7. The value of B_R as a function of $q \equiv \lambda^2 X_b$ for $d = 1$, 2 and 3.

The above relations show that for any dimension d the coefficient B_R is only a function of q which, according to equation (62) and using that $\tilde{\rho}_s = 1/\lambda^2$, is equal to $X_b/\tilde{\rho}_s$. The smaller $X_b/\tilde{\rho}_s$, the smaller B_R, and the smaller the front velocity (equation (55)). This is a

natural result since the ratio $X_b/\tilde{\rho}_s$ is a measure of how much growth substance has to be supplied by diffusion. The smaller this ratio, the more time it will take to grow an aggregate of a given radius. It is also an important result because it gives a direct relation between the front velocity $v(t)$, the bulk concentration X_b and the solid-phase density $\tilde{\rho}_s$. This implies that for a given X_b, one can determine $\tilde{\rho}_s$ by measuring $v(t)$ or $R(t)$ without knowing $\hat{v}$ and α. This result, which is in a sense independent of the approximations involved in the derivation of equation (18), forms the basis for the diffusion-limited instability test described in the next section.

Equating the two expressions for the front velocity in the quasi-stationary regime, equations (32) and (55) with $\beta = 1/2$, we find that the coefficient B_v is given by

$$B_v = \left(\frac{2X_b\lambda}{B_R}\right)^2. \tag{73}$$

For the case where $\lambda \leqslant 1$, where we have stable growth with $\tilde{\rho}_s = 1$, we can determine B_R and B_Δ by applying the same analysis as for $\lambda > 1$. If we do so, we find exactly the same relations for B_R and B_Δ but with q replaced by X_b. This means that for $\lambda < 1$ the front velocity in the quasi-stationary regime does not depend on λ, but is completely determined by diffusion, which is a known result for diffusion-limited stable growth. However, equation (73) applies for all $\lambda < \sqrt{1/X_b}$, so B_v depends on λ also for $\lambda \leqslant 1$. The smaller λ ($\leqslant 1$), the smaller B_v, and the more time it takes to reach the diffusion-limited regime (where $B_v t \gg 1$).

4. Implications

Several experimental values for a non-dense growth process can be obtained. In some cases we only have the position of the growth front as a function of time, $R(t)$. Other possible data are the averaged solid-phase density $\tilde{\rho}_s$, the growth front width Δ_G and the width of the diffusion layer Δ_D. For (quasi-) two-dimensional systems, $R(t)$, $\tilde{\rho}_s$ and Δ_G can be obtained by optical transmission microscopy. For a three-dimensional system these data may be obtained by confocal scanning laser microscopy (CSLM). The extent of the diffusion field Δ_D can be measured by, for example, optical interferometry [25] or Schlieren microscopy [26].

Sometimes there is uncertainty about whether the observed instability, i.e. the non-dense character of an aggregate, is due to diffusion limitation or to the surface kinetics. For such cases, if the growth has taken place under the condition of a free diffusion layer, it is possible to carry out a simple test, described hereafter as the diffusion-limited instability test, which is based on the measured $R(t)$ data and a known diffusion constant D. At the same time, this test gives an estimate of the averaged aggregation density.

4.1. Diffusion-limited instability test

According to our model, the position of the growth front (in real units) for a structure with a constant (non-fractal) aggregation density should obey the relation

$$R(t) = \sqrt{D}B_R(t_0 + t)^{1/2} \tag{74}$$

where we have chosen the origin of the time axis at a point after the initial collapse of the front velocity, i.e. in the stationary regime. This means that t_0 is an initial time which is at least as large as the time needed to reach the stationary regime. The difference from expression (55) with $\beta = 1/2$ is the factor $\sqrt{D}$, which appears due to the back-transformation to the real time and space coordinates. For measured $R(t)$ data, the coefficient B_R can be obtained from the slope s of the best straight-line fit of the data in an R^2 versus t plot according to $B_R = \sqrt{s/D}$.

Then, if we insert B_R into one of the equations (66), (68) or (69), depending on the geometrical dimension d, we have an equation for q that can be solved for q. Alternatively, one can also use figure 7. Consequently, for a given X_b the instability parameter λ can be obtained via equation (62). Then there are two possibilities:

(i) $\lambda \leqslant 1$. In this case the observed instability is not due to diffusion limitation, but must be due to the surface kinetics (e.g. polymer spherulites). According to our model, only the stable steady-state solution (43), yielding $\tilde{\rho}_s = 1$, would apply. Apparently the diffusion-limited regime has not yet been reached, and our model does not give any further quantitative information. However, in the language of our model one could say that for these cases both $\hat{v}$ and α are small. A small $\hat{v}$ means that the diffusion-limited regime can only be reached for very long times and large systems. Hence, the observed instability is caused by a small lateral growth factor α and not by diffusion limitation.

(ii) $\lambda > 1$. This means that at the observed front velocity the mass transport is a limiting factor for the averaged solid-phase density, since according to equation (42) $\tilde{\rho}_s = 1/\lambda^2$ is less than unity in this case. Whether the surface kinetics represents an additional limiting factor, with the result that the actual averaged density is less than $1/\lambda^2$, cannot be decided on the basis of the $R(t)$ data only. In fact this depends on whether the diffusion-limited regime has been reached or not. If one is able to determine that the width of the growth front, Δ_G, is substantially smaller than R, then one can conclude that the diffusion-limited regime applies and $1/\lambda^2$ is an estimate for the averaged solid-phase density.

In some cases the growth of a non-dense structure may take place in the diffusion-limited regime, but the front position does not agree with equation (74) in the sense that the exponent in the time dependence is larger than $1/2$. Usually one expects it to be between 1/2 and 1. A possible explanation for this could be that the actual solid-phase density is not constant but decreases (weakly) as a function of r, eventually according to some fractal dimension $D_H < d$. This yields a less quickly decreasing front velocity since fewer growth units have to be supplied as compared to the case where the solid-phase density would remain constant. However, if the exponent is approximately equal to one, i.e. $R(t) \propto t$, then it is also possible that the value of q is close to one, which means that $\tilde{\rho}_s$ is equal to the bulk concentration X_b. In this case, mass transport is not a limiting factor and, as a consequence, the front velocity is constant. Note that also structures with a decreasing aggregation density will reach the limit value $\tilde{\rho}_s = X_b$ for sufficiently long growth times. In both cases the above test can still be carried out. For weakly decreasing $\tilde{\rho}_s$, equation (74) still applies but with a weakly time-dependent $B_R = B_R(t_0 + t)$. The test will lead to a time averaged value for B_R, and consequently gives an averaged value for λ and $\tilde{\rho}_s$.

Actually, it is possible to extend the theory to describe also fractal growth, by assuming a time-dependent parameter $\alpha(t)$ (and/or eventually a time-dependent parameter $\tilde{K}_{\|}(t)$) [24]. Assuming that the solution of the NDG equations for (weakly) time-dependent parameters can be described as a gradual evolution of the solution for constant parameters, one finds that, for a given power-law behaviour of

$$\lambda(t) \equiv \sqrt{\frac{\hat{v}(t)a_{\|}}{\alpha(t)D}}$$

as a function of t, the power behaviour of $\tilde{\rho}_s(r)$ as a function of r and that of $R(t)$ as a function of t are fixed. This implies that one can determine the fractal dimension of a structure by the determination of the exponent β from measured $R(t)$ data.

Nevertheless, the diffusion-limited instability test should not be applied to very open needle-like structures with a low fractal dimension, since such structures are not described by

the NDG equations. It should be applied to structures which look like having either a constant or weakly decreasing aggregation density.

4.2. Solid-phase density and width of the growth front

If the averaged solid-phase density, $\tilde{\rho}_s$, is also available experimentally, one can compare this with the estimate that follows from the diffusion-limited instability test. This gives additional information on the growth mechanism.

As mentioned above, a strong indication for diffusion limitation is obtained by measuring the width of the growth front, Δ_G, which must be smaller than R in the diffusion-limited regime. Besides, if Δ_G is constant during the growth, this indicates that also $\tilde{\rho}_s$ is constant (equations (42) and (52)). From the measured Δ_G, the parameters α and $\hat{v}$ can be determined as follows.

The growth front in real units is given by

$$\Delta_G = \sqrt{\frac{Da_\parallel}{\alpha \hat{v}}}\,\Delta'_G \tag{75}$$

where Δ'_G is the front width in the dimensionless units given by equation (52). Then by substitution of equation (52) into (75) and using equation (28), we find that α is given by

$$\alpha = \frac{a_\parallel}{\Delta_G}[1 + \ln(\exp(-1)\tilde{\rho}_s + 1 - \tilde{\rho}_s)]. \tag{76}$$

We recall that α is related to the averaged thickness of the branches and the ratio $K_\perp/K_\parallel$ by equations (10) and (13), so the determination of α by the measurement of the front width may lead to useful information on $K_\perp$ if an estimate of the averaged thickness of the branches is available. Note that $K_\perp$ also includes the rate of formation of side branches.

Finally, by combination of equation (28) and equation (76) we find the following expression for $\hat{v}$:

$$\hat{v} = \frac{D\lambda^2}{\Delta_G}[1 + \ln(\exp(-1)\tilde{\rho}_s + 1 - \tilde{\rho}_s)] = \frac{D}{\Delta_G \tilde{\rho}_s}[1 + \ln(\exp(-1)\tilde{\rho}_s + 1 - \tilde{\rho}_s)] \tag{77}$$

where in the latter step we have used equation (42), neglecting the second term which is permitted for a free diffusion layer. In particular, equation (77) is a useful relation when good estimates for $\hat{v}$ are available, since in that case we have a direct relation between the front width and the averaged solid-phase density.

For a free diffusion layer, a given solid-phase density $\tilde{\rho}_s$ and width of the growth front Δ_G, the parameters $\hat{v}$ and α are uniquely fixed by the two equations (42) (with $\tilde{X}_R$ neglected) and equation (76), after elimination of λ by using equation (28). The same is also true for a given fixed diffusion layer where $\tilde{X}_R$ follows from equation (45). This illustrates the applicability of our model as a phenomenological description for non-dense growth. It gives a clear and relatively simple parametrization of such growth and can be used to obtain a qualitative and quantitative understanding of these complicated processes.

5. Summary and discussion

We have presented a continuum description of diffusion-limited non-dense growth which can be used for a qualitative and quantitative analysis of an experimentally observed unstable growth process, in particular for those with a non-fractal scaling behaviour of the aggregation density. By applying an averaging procedure, the spatial dimension in the model equations is reduced to one, which makes the problem much easier to solve. The price for this reduction

is that the equations contain one parameter (α) which is not related to the microscopic kinetic processes at the surface in a direct manner, so it cannot be determined easily *a priori* from known data for a given system. Therefore the model should be used in combination with experimental data.

The instability is characterized by one parameter, the instability parameter λ, which is directly related to the aggregation density. A large λ gives an open structure with a small solid-phase density, whereas a small λ gives a dense structure. The influence of the boundary conditions in the liquid outside the aggregate on the aggregation density $\tilde{\rho}_s$ is limited if the width of the diffusion layer is large, but a significant increase of $\tilde{\rho}_s$ can occur for a small fixed diffusion layer and a high concentration of growth units in the bulk liquid. A fixed diffusion layer yields a constant steady-state front velocity, whereas a free diffusion layer results in a front velocity which is proportional to $\sqrt{D/t}$ in the diffusion-limited regime. In the latter case we have also determined the proportionality constant ($B_R/2$), which turns out to be a function of the ratio between the liquid bulk concentration and the averaged solid-phase density. For a given $\tilde{\rho}_s$ this result is independent of the details of the surface kinetics taking place within the growth front and is the basis of a simple test which can be carried out for given front velocity data and diffusion constant in order to find out whether the non-dense character of the growth is due to diffusion limitation. In the latter case the test also gives the aggregation density.

In our model the surface kinetics is represented by two parameters, $\hat{v}$ and α. These two parameters, together with the diffusion constant and the size of the growth units, have a direct relationship with the solid-phase density and the width of the growth front. An estimate of $\hat{v}$ may be available, but most probably α is not known *a priori* for a given system. It would be a challenge to try to find a direct theoretical approach for the determination of α. One may think of minimizing the total free energy, which would lead to an estimate of the averaged thickness of the branches giving α_b by equation (10). In that case, estimates of the bulk and surface free energies of the solid phase are needed. Another possibility is to extend the model such that the two forms of lateral growth, namely the thickening of the branches and the formation of side branches, are taken into account separately. A fast formation of side branches leads to relatively thin branches, i.e. large α, yielding denser structures. This approach would amount to including one extra differential equation, describing the evolution in time of α. This may lead to a non-constant $\alpha(t)$ in the diffusion-limited regime, which would give rise to solutions with a fractal or non-constant scaling behaviour.

Acknowledgment

This work was sponsored by Unilever Research Vlaardingen, The Netherlands.

References

[1] Mullins W W and Sekerka R F 1963 *J. Appl. Phys.* **34** 323
Mullins W W and Sekerka R F 1964 *J. Appl. Phys.* **35** 444
[2] Kassner K and Brener E 1994 *Phys. Rev.* E **50** 2161
[3] Langer J S and Müller-Krumbhaar H 1978 *Acta Metall.* **26** 1681
[4] Langer J S and Müller-Krumbhaar H 1983 *Phys. Rev.* A **26** 127
[5] Vicsek T 1984 *Phys. Rev. Lett.* **53** 2281
[6] Glicksmann 1983 *Handbook of Crystal Growth* vol 1b, ed D T J Hurle (Amsterdam: Elsevier)
[7] Keith H D and Padden F J 1963 *J. Appl. Phys.* **34** 2409
[8] Keith H D and Padden F J 1964 *J. Appl. Phys.* **35** 1270
[9] Schultz J M 1991 *Polymer* **32** 3268
[10] Benard A and Advani S G 1996 *Polym. Eng. Sci.* **36** 520

[11] Witten T A and Sander L M 1981 *Phys. Rev. Lett.* **47** 1400
[12] Meakin P 1983 *Phys. Rev.* A **27** 604
[13] Eden M 1961 *Proc. 4th Berkeley Symp. on Mathematical Statistics and Probability* vol 4, ed J Neyman (Berkeley, CA: University of California Press) p 123
[14] Witten T A and Sander L M 1983 *Phys. Rev.* B **27** 5686
[15] Vos R F 1984 *Phys. Rev.* B **30** 334
[16] Tang C 1985 *Phys. Rev.* A **31** 1977
[17] Eckmann J P, Meakin P, Procaccia I and Zeitak R 1989 *Phys. Rev.* A **39** 3185
[18] Meakin P, Family F and Vicsek T 1987 *J. Colloid Interface Sci.* **117** 394
[19] Xiao R F, Alexander J I D and Rosenberger F 1989 *Phys. Rev.* A **39** 6397
[20] Krukowski S and Rosenberger F 1994 *Phys. Rev.* B **39** 12 464
[21] Krukowski S and Tedenac J C 1996 *J. Cryst. Growth* **160** 167
[22] Price F P 1960 *J. Polym. Sci.* **42** 49
[23] Hoffman J D, Davis G T and Lauritzen J I 1976 *Treatise on Solid State Chemistry* vol 3, ed N B Hannay (New York: Plenum) p 497
[24] Los J, Bennema P, van Enckevort W J P and Hollander F A 2000 work in progress
[25] van Enckevort W J P 1995 *Curr. Top. Cryst. Growth Res.* **2** 535
[26] Kleine S, van Enckevort W J P and Derix J 1997 *J. Cryst. Growth* **179** 240